

## THE EFFECT OF POLYANILINE ON THE CHARACTERIZATION OF ALGINATE/CARRAGEENAN/POLYANILINE FILM LOADED WITH LOVASTATIN

Nguyen Thi Nga<sup>1</sup>, Pham Nguyen Thao Nguyen<sup>2</sup>, Bui Thanh Nga<sup>2</sup>, Nguyen Ngoc Hai<sup>2</sup>, Huynh Xuan Mai<sup>2</sup>, Vu Minh Hang<sup>2</sup>, Nguyen Thi Hoai Thuong<sup>2</sup>, Vu Quoc Manh<sup>3</sup>, Le Van Dat<sup>4</sup> and Vu Quoc Trung<sup>2,\*</sup>

<sup>1</sup>Hanoi Medical College, Hanoi, Vietnam

<sup>2</sup>Hanoi National University of Education, Ha Noi, Vietnam

<sup>3</sup>Thanh Do University, Ha Noi, Vietnam

<sup>4</sup>Lam Son High School for Gifted Students, Thanh Hoa, Vietnam

\*Corresponding author: Vu Quoc Trung, email: [trungvq@hnue.edu.vn](mailto:trungvq@hnue.edu.vn).

Received March 26, 2026. Revised April 28, 2026. Accepted: June 30, 2026.

**Abstract.** Lovastatin (Lov), a potent inhibitor of 3-hydroxy-3-methylglutaryl coenzyme A (HMG-CoA) reductase, has limited clinical utility because of its poor aqueous solubility and suboptimal pharmacokinetics, characterized by low oral bioavailability (<5%) and a short elimination half-life. To overcome these limitations, a novel pH-responsive drug delivery system was developed by integrating the conductive polymer polyaniline (PANi) into a natural biopolymer matrix of sodium alginate (Alg) and  $\kappa$ -carrageenan (Carr). A series of Lov-loaded alginate/carrageenan/polyaniline/lovastatin (ACPL) biocomposite films containing different PANi content (3–15% w/w) were prepared by in situ oxidative polymerization and solvent casting. Structural and thermal characterization through Fourier transform infrared spectroscopy (FTIR), field emission scanning electron microscopy, and differential scanning calorimetry confirmed that lovastatin was successfully stabilized within the ternary matrix through an intermolecular network of hydrogen bonding and van der Waals interactions, effectively preserving its chemical integrity while disrupting its crystalline lattice. Morphological analysis revealed that the incorporation of PANi significantly refined the drug's particle size from a micro-scale (10–60  $\mu\text{m}$ ) to a sub-micron dispersion (0.05–0.20  $\mu\text{m}$ ), with the ACPL5–alginate/carrageenan/polyaniline/lovastatin formulation, incorporating 5% polyaniline relative to the alginate/carrageenan polymer matrix, exhibiting the most homogeneous distribution. In vitro release studies demonstrated superior site-specific performance; all formulations provided robust gastric protection at pH 2.0 (release <10%), while ACPL5 achieved a near-quantitative sustained release of 97.53% at pH 7.4 within 30 h. These results demonstrate that the Alg/Carr/PANi composite, particularly at a 5% PANi loading, is a highly effective vehicle for modulating release kinetics and potentially enhancing the therapeutic efficacy of hydrophobic statins.

**Keywords:** alginate/carrageenan/PANi, lovastatin, biocomposites, drug delivery.

## 1. Introduction

Lovastatin (Lov), the first statin approved for clinical use, is predominantly biosynthesized via fermentation of the filamentous fungus *Aspergillus terreus* [1]. Its industrial manufacture via submerged fermentation offers significant economic advantages [2]. However, its clinical utility is limited by unfavorable pharmacokinetic properties, including low oral bioavailability (<5%) and a short elimination half-life (1–2 h), resulting in suboptimal systemic exposure [3].

To enhance bioavailability, a key pharmaceutical objective is to improve solubility and modulate release kinetics through advanced polymeric delivery systems. Natural biopolymers like carrageenan (Carr) and alginate (Alg) are widely utilized for this purpose. Concurrently, the conductive polymer polyaniline (PANi) has attracted increasing attention for its "smart," stimuli-responsive characteristics and potential as a biocompatible scaffold [4]. The integration of such polymers has been extensively documented. For example, Gemma Leone *et al.* (2016) used  $\kappa$ -carrageenan/gellan gum formulations to enhance lovastatin delivery from Red Yeast Rice, demonstrating that composite matrices (e.g., 40/60, 50/50 ratios) facilitated enhanced drug release and improved hypocholesterolemic effect [5]. Suhair *et al.* reported a fivefold increase in Lov dissolution via encapsulation in Eudragit L100 microparticles [6]. Kelly A. Langert *et al.* engineered PLGA nanoparticles for Lov, proposing a localized delivery strategy for inflammatory demyelinating diseases [7]. Beyond these, PANi has emerged as a promising component in drug delivery systems. Zhang *et al.* demonstrated that higher molecular weight PANi exhibited reduced cytotoxicity [8]. Subsequent PANi-based composites have been used for controlled delivery of curcumin [7], safranin [8], and indomethacin [9]. Hussein Shokry *et al.* developed electroactive PLA-PANi/silica hybrid scaffolds for targeted release [10], while Yang *et al.* synthesized GO/Fe<sub>3</sub>O<sub>4</sub>/PANi nanoparticles for stimuli-responsive chemotherapeutic delivery [11]. A strategy to improve biocompatibility involves combining natural and synthetic polymer systems. Minisy *et al.* fabricated chitosan/PANi nanofibers exhibiting pH-dependent release of ketoprofen [12]. Similarly, Thach Thi Loc *et al.* [13] developed AgI/Cs/Lov films compatibilized with PEO or PCL to regulate drug release kinetics. This approach aligns with the broader trend of multifunctional biopolymer composites, exemplified by Viteri *et al.*, who designed an intelligent magnetic chitosan/agarose hydrogel for sustained, pH-dependent doxorubicin release [14].

Most published investigations on lovastatin release have predominantly focused on particulate formulations, wherein the drug is liberated via a surface dissolution mechanism. In contrast, film-based matrices offer advantages in terms of controlled matrix swelling, tunable thickness, and ease of fabrication, which are particularly suited to sustained, pH-responsive delivery applications.

To the best of our knowledge, a Lov-loaded composite integrating Carr, Alg, and PANi has not yet been reported. Therefore, this study aims: (i) to synthesize and characterize a series of lovastatin-loaded carrageenan/alginate/PANi composites with varied PANi content (3-15% w/w); and (ii) to evaluate the effect of PANi content on the drug release profile under physiologically relevant conditions (pH 2.0 and 7.4).

## 2. Materials and methods

### 2.1. Chemicals and synthesis

#### 2.1.1. Chemicals

Lovastatin (Lov, purity  $\geq 98\%$ ) was sourced from Rhawn (China). Carrageenan powder (purity  $\geq 95\%$ ), sodium alginate, ammonium persulfate (APS), and aniline (liquid) were procured from Aladdin Co., Ltd. (China). Other analytical or reagent-grade chemicals, including acetic acid, absolute ethanol, hydrochloric acid, potassium chloride, sodium hydroxide, and potassium dihydrogen phosphate, were used as received.

#### 2.1.2. Synthesis of Lov-carrying Alg/Carr/PANi biocomposites with variable content of PANi

*Table 1. Symbols and compositions of the ACPL composite samples*

No.	Symbols	Alg (g)	Carr (g)	Lov (g)	Aniline (mL)	APS (g)
1	ACPL0	0.80	0.20	0.10	0.00	0.000
2	ACPL3	0.80	0.20	0.10	0.03	0.075
3	ACPL5	0.80	0.20	0.10	0.05	0.125
4	ACPL7	0.80	0.20	0.10	0.07	0.175
5	ACPL10	0.80	0.20	0.10	0.10	0.250
6	ACPL15	0.80	0.20	0.10	0.15	0.375

The study of Alg/Carr/PANi/Lov composites was kept constant in the composition of the biopolymers and drug, varying only the PANi content to investigate the influence of the conductive polymer (PANi) on the lovastatin-loaded Alg/Carr delivery system. The specific preparation procedure was as follows. First, 0.8 g of Alg was dissolved in 50 mL of distilled water at 40 °C for 30 minutes to obtain a homogeneous solution A. Simultaneously, 0.2 g of Carr was added to 40 mL of distilled water (at a Carr/water ratio of 1/200 g/mL) at 80 °C for 30 minutes, forming a second homogeneous solution B. Solutions A and B were mixed using a homogenizer at 20,000 rpm for 5 min to form mixture C. Mixture C was stirred magnetically in a 250 mL beaker for 1.5 hours, yielding mixture D. Next, aniline was added to mixture D and stirred for 30 minutes. Subsequently, APS (at a molar APS/aniline ratio of 1/1) was added, and stirring continued for 1 hour, resulting in solution K [15]. Separately, Lov was dissolved in C<sub>2</sub>H<sub>5</sub>OH using a heated magnetic stirrer to prepare drug solution E. Solution E was loaded into a glass burette and added dropwise into solution K under continuous homogenization at 20,000 rpm, producing dispersion F. Dispersion F was magnetically stirred for 1.5 hours. It then underwent two cycles of homogenization (5 min each) followed by two cycles of magnetic stirring (5 min each). The final mixture was poured into petri dishes (diameter 90 mm) at a fixed volume of approximately 30 mL per dish to yield a wet film of controlled thickness. After solvent evaporation and drying in an oven at 40 °C for 48 hours, the resulting dry films had a uniform thickness of approximately 0.3 - 0.4 mm, as verified by digital micrometer measurements at five positions across each film. The resulting drug-loaded

films were stored in zip-lock bags under suitable conditions for subsequent analytical characterization [9]. The symbols and compositions of the ACPL composite samples are presented in Table 1.

## 2.2. Characterization of the ACPL biocomposites

Fourier-transform infrared (FTIR) spectroscopy was performed using a Nexus 670 spectrometer to identify characteristic functional groups, with spectra recorded across the wavenumber range of 400 - 4000  $\text{cm}^{-1}$ . Drug quantification during release studies was conducted via ultraviolet-visible (UV-Vis) spectroscopy on a UV-1900 spectrophotometer, using calibration curves within the wavelength range of 200 - 400 nm. Sample morphology was examined by scanning electron microscopy (SEM) using a Hitachi S-4800 instrument, with specimens sputter-coated with a thin layer of platinum prior to imaging. Thermal properties were assessed by differential scanning calorimetry (DSC) on a DSC60 instrument; samples were heated from ambient temperature to 300 °C at a constant rate of 10 °C/min under a continuous nitrogen purge. The thickness of each film sample was measured using a digital micrometer screw gauge at five different positions, and the average value was recorded. The film thickness of all samples was maintained at approximately 0.3 - 0.4 mm. All acquired data were processed and analyzed using Microsoft Excel software.

## 2.3. Study of drug release

The in vitro drug release profile of lovastatin from the ACPL composites was evaluated under simulated physiological conditions. Experiments were conducted separately in buffer solutions mimicking the gastric (pH 2.0) and intestinal (pH 7.4) environments, maintained at  $37.0 \pm 0.1$  °C. A precisely weighed amount of each composite was introduced into 200 mL of the respective release medium under continuous agitation. At predetermined hourly intervals, 5 mL aliquots were withdrawn and replaced with an equal volume of fresh buffer to preserve sink conditions throughout the study. The concentration of released lovastatin in each aliquot was determined by measuring its absorbance and interpolating the value using previously constructed calibration curves. The calibration equations were  $y = 2598.2x - 0.1468$  ( $R^2 = 0.9972$ ) for pH 2.0 and  $y = 3978x - 0.1975$  ( $R^2 = 0.9985$ ) for pH 7.4. To ensure reliability, each release experiment was conducted in triplicate.

$$H(\%) = \frac{m}{m_0} \cdot 100\%$$

where, H: Cumulative lovastatin release at the investigated time point (%).

m: Mass of lovastatin released at the investigated time point.

$m_0$ : Initial mass of lovastatin.

## 3. Results and discussion

### 3.1. FTIR spectrum of the lovastatin-loaded ACPL composites

The FT-IR spectra (Figure 1, Table 2) of pure lovastatin and ACPL composites confirmed the structural integrity of all components. Characteristic bands of Lov were

clearly identified: O–H stretching at  $3544\text{ cm}^{-1}$ , C–H stretching of  $-\text{CH}_3$  and  $-\text{CH}_2$  groups at  $2965$ ,  $2929$ , and  $2807\text{ cm}^{-1}$ , and a prominent C=O peak at  $1700\text{ cm}^{-1}$ . The retention of these bands with only minor shifts in the composite spectra confirms that the lovastatin structure remained intact after incorporation into the polymer matrix [15], [16]. Characteristic absorption peaks of alginate, carrageenan, and PANi were also detectable across all ACPL samples, including a broad O–H/N–H stretching band in the  $2920\text{--}3300\text{ cm}^{-1}$  region, C–O stretching of polysaccharides in the  $1000\text{--}1300\text{ cm}^{-1}$  range, and C–H stretching near  $2900\text{ cm}^{-1}$  [15], [16]. The observed peak shifts, without the formation of new covalent bonds or disappearance of existing functional groups, indicate that intermolecular interactions – primarily hydrogen bonds and van der Waals forces – govern the composite structure. These bonds form between the  $-\text{COO}^-/-\text{OH}$  groups of alginate,  $-\text{C}-\text{O}/-\text{OH}$  groups of carrageenan,  $-\text{NH}$  groups of PANi, and  $-\text{C}=\text{O}/-\text{OH}$  groups of lovastatin [15], [16]. The absence of free  $-\text{NH}_2$  stretching peaks from the aniline monomer confirms complete polymerization into PANi. Overall, the FTIR results demonstrate that Alg, Carr, PANi, and Lov are physically combined without structural modification, ensuring that the pharmacological activity and chemical integrity of lovastatin are preserved within the composite carriers.

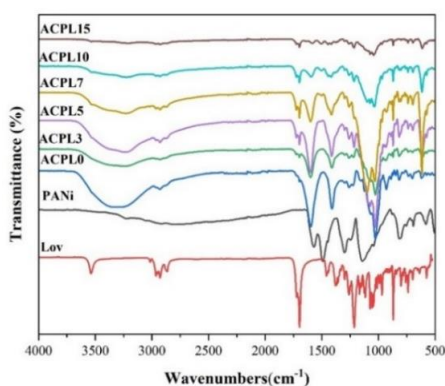


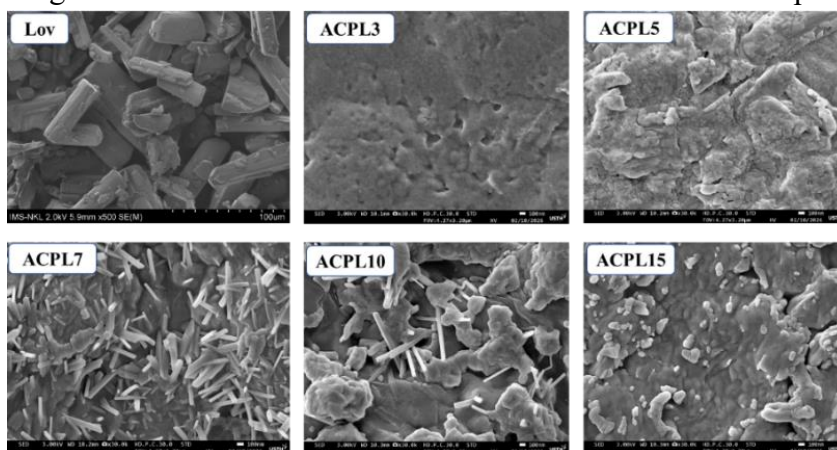
Figure 1. FTIR spectra of Lov and ACPL composite

Table 2. Characteristic wavenumbers of Alg, Carr, PANi, Lov, and ACPL samples ( $\text{cm}^{-1}$ )

	Alg	Carr	Lov	PANi	ACPL0	ACPL3	ACPL5	ACPL7	ACPL10	ACPL15
$\nu_{\text{OH}}$ , $\nu_{\text{NH}_2}$ , $\nu_{\text{NH}}$	3350	3380	3644	3436	3247	3250	3245	3255	3260	3257
$\nu_{\text{C}=\text{N}}$	-	-	-	1560	1567	1565	1568	1570	1562	1569
$\nu_{\text{C}=\text{C}}$ (arene)	-	-	-	1483	1487	1485	1488	1486	1482	1487
$\nu_{\text{CH}}$	2930	2935	2966	2867	1926	2928	2925	2927	2930	2925
$\nu_{\text{C}=\text{O}}$	1710	-	1696	-	1713	1710	1715	1712	1708	1711
$\delta_{\text{NH}}$	-	-	-	1600	1589	1595	1590	1585	1588	1592
$\delta_{\text{CH}}$	1415	1375	-	1097	1421	1420	1418	1415	1422	1419
$\nu_{\text{C}-\text{O}-\text{C}}$	1030	1065	1071	-	1029	1025	1035	1040	1032	1028

### 3.2. Morphology of the lovastatin-loaded ACPL composites

FESEM analysis revealed that pure lovastatin exhibited a rod-like crystalline morphology with large, non-uniform particles ranging from 10 to 60  $\mu\text{m}$ . In contrast, all ACPL composite samples showed dramatically reduced particle sizes (0.05 - 0.2  $\mu\text{m}$ ) with homogeneous dispersion within the polymeric matrix. The ACPL0 sample (without PANi) displayed noticeably larger particles than PANi-containing formulations, confirming that lovastatin dispersibility is directly dependent on PANi content. This enhanced dispersion is driven by hydrogen bonding between the  $-\text{CO}$  and  $-\text{NH}_2$  groups of the Alg/Carr/PANi matrix and the  $-\text{OH}$  groups of lovastatin, promoting efficient drug-polymer binding and uniform distribution within the three-dimensional composite network.



*Figure 2. DSC diagrams of Lov and ACPL composites*

Among all formulations, ACPL5 exhibited the most favorable morphology, with spherical, uniformly distributed lovastatin particles of 0.05–0.08  $\mu\text{m}$ . This optimum is explained by the PANi concentration-dependent network formation: at low PANi contents (ACPL0, ACPL3), the underdeveloped network provides insufficient anchoring sites, allowing drug aggregation into larger particles; at high PANi loadings (ACPL7–ACPL15), hydrophobic PANi chain aggregation disrupts matrix homogeneity and promotes uncontrolled drug clustering. ACPL5 achieves the ideal balance between adequate network density and the absence of hydrophobic aggregation, resulting in superior lovastatin dispersion.

In this study, the film thickness of all samples was maintained at comparable values (approximately 0.3 - 0.4 mm), with the sole variable being the concentration of polyaniline within each formulation. This experimental design was implemented to elucidate the correlation between lovastatin release behavior and polyaniline content, while minimizing potential confounding effects arising from variations in other experimental parameters.

### 3.3. Thermal properties of the lovastatin-loaded ACPL composites

The DSC thermogram of pure lovastatin showed a single sharp endothermic peak at 174.6  $^{\circ}\text{C}$ , corresponding to its melting point. In contrast, all ACPL composite samples exhibited two distinct endothermic transitions: the first at a lower temperature attributed

to dehydration of the polymeric matrix (alginate, carrageenan, and PANi), and the second corresponding to lovastatin melting within the composite. The melting point of lovastatin in all ACPL formulations was significantly lower than that of the pure drug, with a progressive decrease observed as PANi content increased from ACPL0 to ACPL15.

**Table 3. DSC parameters obtained with Lov and ACPL composites**

Samples	1st endothermic peak (°C)	2nd endothermic peak (°C)
Lov	-	174.6
ACPL0	83.5	172.5
ACPL3	65.0	171.0
ACPL5	68.0	154.5
ACPL7	48.0	173.0
ACPL10	74.0	166.0
ACPL15	63.0	171.5

This behavior is attributed to intermolecular hydrogen bonding between lovastatin and the functional groups of the polymeric components, disrupting the drug's crystalline lattice. The reduction in particle size, confirmed by FESEM analysis, further contributes to this melting point depression, as smaller crystals with higher surface energy tend to melt at lower temperatures. PANi facilitates the formation of a three-dimensional network that promotes uniform drug dispersion and prevents recrystallization. Among all formulations, ACPL5 exhibited the lowest lovastatin melting point, consistent with its optimal morphological characteristics observed by FESEM, indicating maximum drug-polymer interactions and the most homogeneous drug dispersion within the composite matrix.

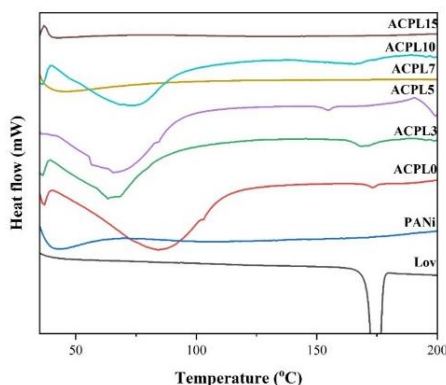


**Figure 3. DSC diagrams of Lov and ACPL composites**

### 3.4. Lovastatin release from ACPL composites

The release profiles of lovastatin (Lov) from ACPL composites were evaluated in simulated gastric fluid (SGF, pH 2.0) and simulated intestinal fluid (SIF, pH 7.4), as illustrated in Figure 4. A biphasic release pattern was observed at pH 7.4: an initial burst release attributed to rapid dissolution of surface-localized Lov particles, followed by a sustained release phase driven by matrix swelling and diffusion of drug molecules from

the polymer network [15]. After 30 hours, cumulative release ranged from 61.6% to 99.9%, with formulations ACPL5, ACPL10, and ACPL15 exceeding 97%. In contrast, at pH 2.0, all formulations demonstrated minimal release (2.7–9.6%), with ACPL0, ACPL5, and ACPL10 achieving less than 5%, confirming effective gastric protection [17], [18]. The ACPL5 formulation exhibited the most favorable dual-functional performance: minimal release at pH 2.0 and maximal release at pH 7.4, ensuring drug protection in the stomach while promoting intestinal absorption [16], [17]. This behavior reflects the structural role of PANi content in network formation. At low PANi concentrations (ACPL0, ACPL3), the incompletely developed matrix creates a porous, poorly stabilized structure that promotes burst release and inadequate kinetic control [15], [18]. At excessive PANi loadings (ACPL7–ACPL15), hydrophobic chain aggregation creates densely packed regions that obstruct diffusion pathways, slowing and limiting overall drug release. The ACPL5 formulation represents the optimal balance, establishing a homogeneous, well-integrated network that enables precise release control through hydrogen bonding and van der Waals interactions between Lov and the polymer components.

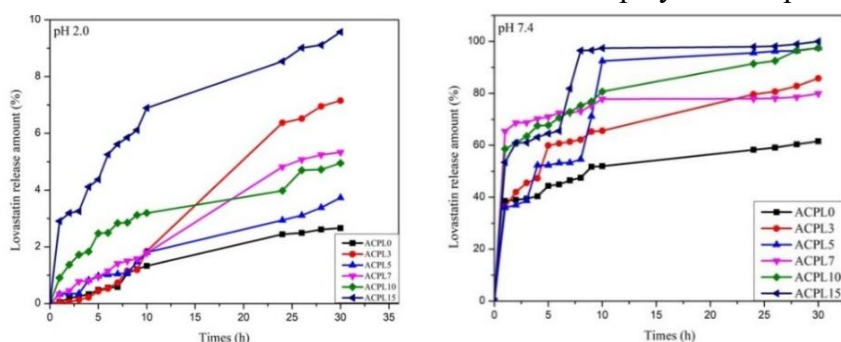


**Figure 4. Plots of time-dependent Lov amounts released from ACPL composites at pH 2.0 and pH 7.4**

#### 4. Conclusions

The developed lovastatin-loaded Alginate/Carrageenan/Polyaniline drug delivery system represents an initial step toward integrating natural biopolymers with a conductive polymer for pH responsive drug delivery. The results demonstrated that PANi incorporation influenced the microstructure of the polymer matrix and modulated the release behavior of lovastatin. Among the formulations investigated, sample ACPL5 stands out for its superior performance, demonstrating excellent intestinal release (97.53%) and effective gastric protection (3.73%). This positions it as a highly promising candidate, paving the way for the future development of advanced drug carrier systems. It should be noted that this study did not include measurements of electrical conductivity or drug release experiments under applied current stimulation. Consequently, the electroresponsive “smart” functionality of PANi within this composite system has not been directly demonstrated and remains to be validated. Future work is recommended along three directions: (i) in vitro and in vivo pharmacological studies, (ii) continuous evaluation of PANi electrical conductivity and its correlation with PANi content, and (iii) drug release experiments under controlled current stimulation to fully realize the electroresponsive potential of this delivery platform.

**Note for Contributors:**

- Short bio: Nguyen Thi Nga is a doctor and lecturer at Hanoi Medical College, Vietnam. Vu Quoc Trung is an Assoc. Professor at Hanoi National University of Education, Vietnam. Vu Quoc Manh is a doctor and lecturer at Thanh Do University, Vietnam. Le Van Dat is a teacher at Lam Son High School for gifted students, Vietnam. Pham Nguyen Thao Nguyen, Bui Thanh Nga, Nguyen Ngoc Hai, Huynh Xuan Mai, Vu Minh Hang, and Nguyen Thi Hoai Thuong are students at Hanoi National University of Education, Vietnam.

- Author's contributions: Nguyen Thi Nga: conceptualization, methodology; Vu Quoc Trung: supervision, review & editing; Vu Quoc Manh: validation, resources; Le Van Dat: data curation, visualization; Pham Nguyen Thao Nguyen & Bui Thanh Nga: data analysis, writing – original draft; Nguyen Ngoc Hai, Huynh Xuan Mai, Vu Minh Hang & Nguyen Thi Hoai Thuong: investigation, sample preparation.

**Conflict of interest:** The authors declare no conflict of interest.

## REFERENCES

- [1] J. M. Henwood & R. C. Heel, "Lovastatin: a preliminary review of its pharmacodynamic properties and therapeutic use in hyperlipidaemia", *Drugs*, vol. 36, no. 4, pp. 429-454, 1988. DOI: 10.2165/00003495-198836040-00003.
- [2] S. Goswami, A. S. Vidyarthi, B. Bhunia, & T. Mandal, "A review on production of lovastatin and its applications", *International Journal of Biotechnology and Bioengineering Research*, vol. 4, no. 1, pp. 581-588, 2013. DOI: 10.51847/qmz5byr.
- [3] A. W. Alberts, "Discovery, biochemistry and biology of lovastatin", *The American Journal of Cardiology*, vol. 62, no. 15, pp. 10J-15J, 1988. DOI: 10.1016/0002-9149(88)90002-1.
- [4] N. M. Cerqueira, E. F. Oliveira, D. S. Gesto, D. Santos-Martins, C. Moreira, H. N. Moorthy, M. J., Ramos & P. A. Fernandes, "Cholesterol biosynthesis: a mechanistic overview", *Biochemistry*, vol. 55, no. 39, pp. 5483-5506, 2016. <https://doi.org/10.1021/acs.biochem.6b00342>.
- [5] G. Leone, M. Consumi, S. Pepi, S. Lamponi, C. Bonechi, G. Tamasi & A. Magnani, "New formulations to enhance lovastatin release from red yeast rice (RYR)", *Journal of Drug Delivery Science and Technology*, vol. 36, pp. 110-119, 2016. <https://doi.org/10.1016/j.jddst.2016.10.001>.
- [6] S. S. Al-Nimry & M. S. Khanfar, "Preparation and characterization of lovastatin polymeric microparticles by coacervation-phase separation method for dissolution enhancement", *Journal of Applied Polymer Science*, vol. 133, pp. 43277-43286, 2016. <https://doi.org/10.1002/app.43277>.
- [7] K. A. Langert, B. Goshu & J. E. B. Stubbs, "Attenuation of Experimental Autoimmune Neuritis with Locally Administered Lovastatin-Encapsulating PLGA Nanoparticles", *Journal of Neurochemistry*, vol. 140, no. 2, pp. 334-346, 2017. <https://doi.org/10.1111/jnc.13897>.
- [8] Y. Zhang, M. Zhou, C. Dou, G. Ma, Y. Wang, N. Feng, W. Wang & L. Fang, "Synthesis and biocompatibility assessment of polyaniline nanomaterials",

*Journal of Bioactive and Compatible Polymers*, vol. 34, no. 1, pp. 16-24, 2019. <https://doi.org/10.1177/0883911518820499>.

- [9] N. Pramanik, K. Dutta, R. K. Basu & P. P. Kundu, "Aromatic  $\pi$ -conjugated curcumin on surface-modified polyaniline/polyhydroxy alkanoate based 3D porous scaffolds for tissue engineering applications", *ACS Biomater. Sci. Eng.*, vol. 2, no. 12, pp. 2365-2377, 2016. DOI: 10.1021/acsbiomaterials.6b00595.
- [10] H. Shokry, U. Vanamo, O. Wiltshka, J. Niinimäki, M. Lerche, K. Levon, M. Linden & C. Sahlgren, "Mesoporous silica particle-PLA-PANI hybrid scaffolds for cell-directed intracellular drug delivery and tissue vascularization", *Nanoscale*, vol. 7, no. 34, pp. 14434-14443, 2015. DOI:10.1039/c5nr03983e.
- [11] Y. F. Yang, F. Y. Meng, X. H. Li, N. N. Wu, Y. H. Deng, L. Y. Wei & X. P. Zeng, "Magnetic Graphene Oxide-Fe<sub>3</sub>O<sub>4</sub>-PANI Nanoparticle Adsorbed Platinum Drugs as Drug Delivery Systems for Cancer Therapy", *Journal of Nanoscience and Nanotechnology*, vol. 19, no. 12, pp. 7517-7525, 2019. DOI:10.1166/jnn.2019.16768
- [12] I. M. Minisy, N. A. Salahuddin & M. M. Ayad, "In vitro release study of ketoprofen-loaded chitosan/polyaniline nanofibers", *Polymer Bulletin*, vol. 78, no. 10, pp. 5609-5622, 2021. DOI:10.1007/s00289-020-03385-z.
- [13] T. T. Loc, T. Hoang, N. T. Chinh & L. D. Giang, "The effects of the compatibilizers on the lovastatin release form the alginat/chitosan/Lov composite", *Vietnam Journal of Chemistry*, vol. 56, no. 3, pp. 389-395, 2018.
- [14] A. Viteri, M. Espanol, M. P. Ginebra & J. García-Torres, "Tailoring drug release from skin-like chitosan-agarose biopolymer hydrogels containing Fe<sub>3</sub>O<sub>4</sub> nanoparticles using magnetic fields", *Chemical Engineering Journal*, vol. 517, 164214, 2025. DOI: 10.1016/j.cej.2025.164214.
- [15] V. T. T. Thao, N. T. H. Nhung, V. Q. Manh, N. N. Linh, N. T. B. Viet & V. Q. Trung, "Synthesis and characterization of Chitosan/Carrageenan/Polyaniline-based biocomposite as lovastatin carrier and its drug release ability in buffer solutions", *HNUE Journal of Science*, vol. 68, no. 3, pp. 64-74, 2023. <https://doi.org/10.18173/2354-1059.2023-0061>.
- [16] H. M. Hung, V. Q. Manh, V. T. T. Thao, D. T. P. Thuy, P. T. Dung, N. T. B. Viet, D. K. Linh, N. N. Linh, D. T. Y. Oanh, N. T. Chinh, T. Hoang & V. Q. Trung, "Evaluation of the effect of the chitosan/carrageenan ratio on lovastatin release from chitosan/carrageenan based biomaterials", *Vietnam Journal of Chemistry*, vol. 60, no. S1, pp. 72-79, 2022. <https://doi.org/10.1002/vjch.202200078>.
- [17] N. T. K. Thoa, V. Q. Manh, H. M. Hung, V. T. Hanh & V. Q. Trung, "Study on the Effect of Lovastatin on the Release Capacity of Lovastatin from Chitosan/Carrageenan Composite Materials", *National Conference on Earth Sciences and Natural Resources for Sustainable Development (ERSD 2022)*, pp. 1296-1302, 2022 (in Vietnamese).
- [18] V. Q. Mamh, V. T. Thao, D. T. Yen, L. T. Dat, N. N. Linh, N. T. B. Viet, N. D. Dat & V. Q. Trung, "Preparation and characterization of carrageenan/lovastatin biomaterials", *HNUE Journal of Science*, vol. 70, no. 2, pp. 91-101, 2025. DOI: 10.18173/2354-1059.2025-0024.